ON THE QUESTION OF ADEQUATE MODELLING OF STEADY-STATE ROTOR DISC-TILT FOR HELICOPTER MANOEUVRING FLIGHT

Richard van Aalst
Richard van Aalst@student.tudelft.nl

Marilena D. Pavel
M.Pavel@lr.tudelft.nl

Delft University of Technology

Abstract

The goal of the present paper was to understand the effects of different approximations considered in the analytical expressions of rotor disc tilt angles when developing a piloted simulation model for helicopter manoeuvring flight. The paper investigated five cases: 1) a classical formulation of the rotor disc tilt; 2) effects of non-uniform induced velocity distribution along the rotor disc introduced in the form of a dynamic inflow correction factor in the lateral disc-tilt; 3) effects of unsteady flow along the rotor blade introduced in the form of a sweep correction factor in the rotor disc-tilt angles; 4) effects of both sweep and dynamic inflow corrections in the formulae of the rotor disc-tilt; 5) effects of high-order coupling terms included in the analytical expressions of the rotor disc-tilt. The paper developed a six degree-of-freedom (6-dof) non-linear helicopter model and implemented these approximations in the model. With respect to the simulated trimmed flight solution, it was demonstrated that using both sweep and dynamic inflow corrections in the analytical expressions of the rotor disc tilt angles resulted in accounting for the experimentally measured peak of the lateral tilt in the region of low flight velocities. This peak is theoretically still unexplained and the above conclusion suggests that the discrepancy may be searched in both modelling the dynamic inflow and the sweep effects on the rotor blade. Using both sweep and dynamic inflow corrections resulted in overpredicted lateral disc-tilt for trimming at high flight speeds. With respect to the manoeuvring flight simulations, three manoeuvres were performed: a doublet in the longitudinal cyclic, a doublet in the lateral cyclic and the acceleration/deceleration manoeuvre from the ADS-33 standard. It was demonstrated that for a pitch axis manoeuvre, the results are mainly affected by dynamic inflow modelling. For a manoeuvre in the roll axis, the coupling between the longitudinal and lateral plane was important and thus the high-order coupling terms considered in the analytical expressions of the rotor disc-tilt played an important role. For a more elaborate manoeuvre such as acceleration/deceleration, the effects of dynamic inflow correction, high-order coupling terms and sweep correction contributed all to the prediction of the flying parameters.

Notations

v_i Glauert's general induced velocity [-]

v_{i0} Glauert's induced velocity at rotor centre [-]

λ rotor inflow ratio relative to no-feathering plane [-]

ε flapping hinge offset [-]

σ rotor solidity [-]

Ω rotor rotational speed [rad/s]

θ_0 collective pitch angle [rad]

λ_0 dynamic inflow ratio

$\lambda = \mu_z - \lambda_0$ rotor inflow ratio relative to no-feathering plane [-]

λ_D rotor inflow ratio relative to tip path plane [-]

μ_x normalized velocity component along body x-axis [-]

$(x_{FIN}, y_{FIN}, z_{FIN})$ position of vertical fin relative to body axes-system [m]

(x_h, y_h, z_h) position of rotor hub relative to body axes-system [m]

(x_{HS}, y_{HS}, z_{HS}) position of horizontal stabilizer relative to body axes-system [m]

(x_{TR}, y_{TR}, z_{TR}) position of tailrotor relative to body axes-system [m]

μ_y normalized velocity component along body y-axis [-]

μ_z normalized velocity component along body z-axis [-]

θ_{tw} blade twist [rad]

C_l^α blade lift curve slope [rad^{-1}]

θ_{1s} longitudinal cyclic pitch [rad]

θ_{1c} lateral cyclic pitch [rad]

Paper presented at the 28th European Rotorcraft Forum, 17-20 September 2002, Bristol, UK

ϕ Euler roll angle [rad]

θ Euler pitch angle [rad]

$[\omega_x]$ rotation operation matrix [rad/s]

[J] moment of inertia matrix [kg· m^2]

[m] mass matrix [kg]

$\{\overline{E_s}\}$ shaft axes-system [-]

$\{\overline{E_b}\}$ body axes-system[-]

a_0 rotor coning angle [rad]

a_1 longitudinal rotor disc-tilt angle [rad]

b_1 lateral rotor disc-tilt angle [rad]

C_H rotor drag force coefficient in no-feathering plane [-]

C_{HD} rotor drag force coefficient in disc plane [-]

C_Q rotor torque coefficient in disc plane [-]

C_S rotor lateral force coefficient in no-feathering plane [-]

C_{SD} rotor lateral force coefficient in disc plane [-]

$C_{T,\ Elem}$ rotor thrust coefficient calculated with blade-element theory [-]

$C_{T,\ Glauert}$ rotor thrust coefficient calculated with Glauert-theory [-]

C_t rotor thrust coefficient in no-feathering plane [-]

C_{tD} rotor thrust coefficient in disc plane [-]

D blade drag force [N]

dt time step [sec]

F force [N]

g acceleration of gravity [m/s^2]

H main rotor drag force [N]

H_D rotor drag force relative to disc plane [N]

h_{req} required height for pilot model [m]

I_x helicopter moment of inertia about body x-axis [kg m^2]

I_{xz} helicopter product of inertia about body x and z axes [kg m^2]

I_y helicopter moment of inertia about body y-axis [kg m^2]

I_z helicopter moment of inertia about body z-axis [kg m^2]

K Glauert's coefficient [-]

K roll angle gain for pilot model [rad^{-1}]

K_h altitude gain for pilot model [sec^{-1}]

K_{h1} altitude gain for pilot model [sec^{-1}]

K_{hdot} vertical speed gain for pilot model [rad/m/s]

K_{int_ϕ} roll angle integral gain for pilot model [$(rad\cdot s)^{-1}$]

K_{int_h} altitude integral gain for pilot model [rad/(m·s)]

K_{int_vs} vertical speed integral gain for pilot model [m^{-1}]

K_{int_x} longitudinal pos. integral gain for pilot model [rad/m·s^{-1}]

K_{int_y} lateral position integral gain for pilot model [rad/(m·s)]

K_{int_θ} integral pitch angle gain for pilot model [rad·s^{-1}]

K_{int_ψ} yaw angle integral gain for pilot model $[(rad\cdot s)^{-1}]$

K_p roll rate gain for pilot model $[(rad/s)^{-1}]$

K_q pitch rate gain for pilot model [rad/s^{-1}]

K_r yaw rate gain for pilot model $[(rad/s)^{-1}]$

K_{vs} vertical speed gain for pilot model [m/s^{-1}]

K_x longitudinal position gain for pilot model [rad/m]

K_{xdot} longitudinal velocity gain for pilot model [rad/m/s]

K_y lateral position gain for pilot model [rad/m]

K_{ydot} lateral velocity gain for pilot model [rad/m/s]

K_θ pitch angle gain for pilot model [rad^{-1}]

K_ψ yaw angle gain for pilot model [rad^{-1}]

$Lift_{FIN}$ vertical fin lift force [N]

$Lift_{HS}$ horizontal stabilizer lift force [N]

m mass [kg]

m_{bl} blade mass [kg]

p, $\overline{p}$ helicopter roll angular velocity and its non-dimensional value [rad/s]

q, $\overline{q}$ helicopter pitch angular velocity and its non-dimensional value [rad/s]

Q rotor torque relative to disc plane [N]

r, $\overline{r}$ helicopter yaw angular velocity and its non-dimensional value [rad/s]

R rotor radius [m]

ϕ_{req} required roll angle for pilot model [rad]

S main rotor lateral force [N]

S_D rotor lateral force relative to disc plane [N]

T main rotor thrust [N]

T_D rotor thrust force relative to disc plane [N]

T_{TR} tailrotor thrust [N]

u x-component of airspeed (body axes-system) [m/s]

v y-component of airspeed (body axes-system) [m/s]

v_s vertical speed [m/s]

$v_{s\ req}$ required vertical speed for pilot model [m/s]

w z-component of airspeed (body axes-system) [m/s]

x Glauert's r/R [-]

X_{FUS} x-component of fuselage force (body axes-system) [N]

x_{req} required longitudinal position for pilot model [m]

y_{req} required lateral position for pilot model [m]

Z_{FUS} z-component of fuselage force (body axes-system) [N]

θ_{req} required pitch angle for pilot model [rad]

ψ_{req} required yaw angle for pilot model [rad]

Subscripts

MR:	Main Rotor
FUS	Fuselage
HS, ht:	Horizontal Stabilizer
FIN, vt:	Vertical Fin
TR:	Tail Rotor
dp:	disc plane

1. Introduction

The helicopter simulation modelling arrived at a complex sophistication where in many cases good agreement can be shown between theory and experiment. However, there are situations in which the model still revels large discrepancies with respect to the flight test data. Many times, due to its complexity, the blame is put on dynamic inflow modelling. And yet, understanding better which couplings between the degrees of freedom of the model are relevant and to what degree of approximation should they be included in the model would improve the predictions made.

The present paper describes an ongoing effort (see ref. [1]) to improve the understanding of the effects of different approximations made in calculating the rotor disc tilt angles for helicopter trim and manoeuvring flight. The paper investigates two main questions:

1) what are the effects on piloted simulation of different approximations made in the analytical expressions of the rotor disc-tilt angles and,
2) what consequence has on the piloted simulation model a 'sweep correction' included in the lateral rotor disc-tilt.

As concerns the first question, most classical books on helicopters derive simple formulae for the rotor disc-tilt angles a_0, a_1 and b_1 by neglecting high-order coupling terms and concentrating on an adequate picture of the flapping behaviour only on the trim flight (see for example ref. [3]). Reference [11] derived the rotor disc-tilt angles a_0, a_1 and b_1 of a helicopter translating and rotating free in space including high-order coupling terms in pitch, roll and yaw attitude rates. The same reference proposed an ordering scheme yielding to truncated analytical expressions for the disc-tilt with maximum errors of 15% from the complete formulas. It was decided to investigate how these high-order coupling terms affect the piloted simulated flight when performing different manoeuvres with a 6 degree-of-freedom (6-dof) non-linear body model.

As concerns the second question, reference [5] derived simple formulae for calculating the lateral disc-tilt angle b_1 including a 'sweep correction' for the effects of unsteady and swept flow on the helicopter rotor blade. It was decided to investigate more carefully what are the effects of this correction on the piloted simulation flight.

The paper is structured as follows:

- first section describes a 6-degree of freedom (6-dof) model for piloted simulation applications;
- second section defines different approximations that can be used in the 6-dof model to calculate the attitude of the rotor tip-path-plane;
- In order to get a feeling for the problem, the third section presents how these approximations affect the way a pilot flies simple doublet manoeuvres given in longitudinal and lateral cyclic;
- Then, the paper presents what are the effects of the above-named approximations when flying the acceleration/deceleration manoeuvre of the ADS-33 standard;
- Finally, general conclusions are discussed.

2. Background of the Study

Earlier work [ref. 7] performed on the question how many degrees of freedom are needed in models for piloted simulation for helicopters indicated that the results are influenced also by the degree of approximation made in calculating the steady-state rotor disc-tilt angles. It was then shown that, when performing a deceleration manoeuvre with the helicopter, the simulation results are influenced by the high-order coupling terms retained in the rotor disc-tilt formulae (see Fig. 1). Accordingly, it was concluded that care should be expressed in approximating the rotor disc tilt angles for piloted simulation modelling.

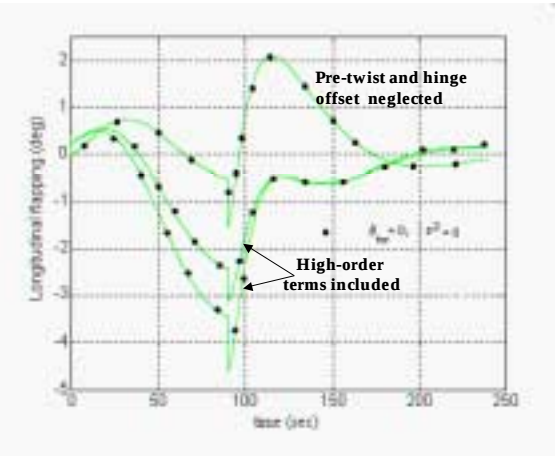

Fig. 1: Longitudinal disc-tilt angle during a deceleration manoeuvre with Bo-105 calculated using different approximations [7]

Furthermore, it is well known that the lateral tilt of the rotor disc in trimmed flight is severely underpredicted when using models in which concepts deriving from the classical lifting line theory are employed. A large part of these discrepancies can be explained when eliminating the rough assumptions made for the induced velocity, namely that this is uniformly distributed over the rotor disc. However, even considering a more realistic distribution it could not yet explain the peak of the lateral tilt obtained experimentally when flying at low velocities (around $\mu = 0.1$, see fig. 2).

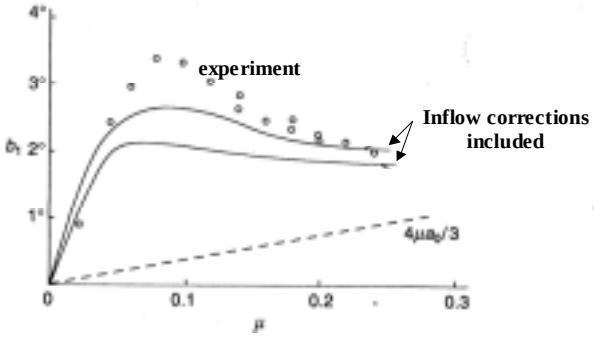

Fig.2: Lateral tilt of the rotor disc; classical theory versus experiment [3]

Reference [5], trying to explain this discrepancy in peak of the lateral rotor disc tilt, argued whether the usual assumption made, i.e. the generation of lift by a blade section depends only on the velocity component perpendicular to the blade span, is not too crude and inconsistent with other approximations used in rotor analyses. Accordingly,, using an improved correction in accounting for the 'sweep effects' on a blade, ref. [5] showed on basis of qualitative arguments that such correction might explain the peak of the lateral rotor disc-tilt at low flight velocities.

It was decided to analyse more systematically and in detail the problem of modelling the rotor disc-tilt [ref. 1]. In this context, the present paper will analyse different approximations made in calculating the rotor disc-tilt angles and how they affect the helicopter behaviour for trimmed and manoeuvring flight.

3. Six Degree-of-Freedom Non-linear Model for Piloted Flight Simulation

3.1. Model Description

A general six degree-of freedom (6-dof) non-linear rigid body model was first developed for piloted time-domain simulations. In a typical 6-dof model the helicopter body is modelled by dividing it into its main components (rotor, fuselage, tailrotor, horizontal stabilizer, vertical fin) and summing the contribution of each part to the general system of forces and moments. The following assumptions are made:

- Aerodynamic forces and moments are calculated using the blade element theory;
- The tail rotor is modelled as an actuator disc;
- The fuselage, horizontal and vertical tails are modelled with linear aerodynamics;
- Rotor disc-tilt dynamics (often the so-called flapping dynamics) is neglected and only steady-state rotor disc-tilt motion is considered;
- The dynamic inflow of both rotor and tail rotor are included in the model as state variables and can be described as a quasi-steady dynamic inflow by means of the time constants of a value between 0.1 to 0.5 sec;
- The rotor is modelled with a centrally flapping hinge;
- No pre-twist or pitch flap coupling are included;
- The lead-lag motion of the blades is neglected;
- The blades are rectangular;
- There are no pitch-flap or pitch-lag couplings;
- There are no tip losses;
- The rotor is placed at the coordinated (x_h, y_h, z_h) from the helicopter centre of mass;
- Gravitational forces are small compared to aerodynamic, inertial and centrifugal forces;
- The flapping and flow angles are small;
- The rotor angular velocity is constant and anticlockwise;
- No reverse flow regions are considered;
- The flow is incompressible;
- The blades have a uniform mass distribution;
- The blade elastic axis, aerodynamic axis, control axis and centre of mass axis coincide.

The following sign conventions are used:

- The longitudinal rotor disc-tilt a_1 is assumed positive when the rotor disc plane tilts backwards;
- The lateral rotor disc-tilt b_1 is assumed positive when the rotor disc plane tilts to the right;
- The longitudinal cyclic is assumed positive when the pilot moves the stick forward;
- The lateral cyclic is assumed positive when the pilot moves the stick to the right.

For a complete derivation of the forces and moments acting on the helicopter components, the reader is referred to references [1], [7], [8] or [10]. The equations of motion describing the motion of the helicopter in the 6-dof model are presented in Appendix A, relations (A2). One may see that these equations depend on the attitude of the rotor disc through the disc-tilt angles a_0, a_1, and b_1. The

present paper will analyse what is the effect of different approximations used to express the disc-tilt angles for flight mechanics applications and how do these approximations affect the pilot's actions during trimmed and manoeuvring flight.

Equations (A2) together with the Euler equations (A3) and the equations of the helicopter trajectory (A4) describe completely the helicopter motion in an inertial system. To fly the helicopter, a Stability Augmentation System (SAS) was implemented. Appendix A, equations A(27) to A(34) describe the four stabilizations functions implemented for each helicopter's control in order to fly it. The 6-dof presented in this paper will be first validated for trim and then used to fly doublets and manoeuvres from the ADS-33 standard.

4. Approximating the Rotor Disc-Tilt Angles for Piloted Simulation Modelling

The flapping motion, as seen from a frame of reference rotating with the blade, can be divided into three distinct time scales:

- fast motions, corresponding to transients associated with the eigenfrequency of the blade;
- intermediate fact motions, corresponding to the steady-state response of the blade to control inputs and body rotations;
- slow motion, corresponding to the steady-state response of the blade to variations of helicopter speed.

Usually, for piloted simulation modelling, one concentrates on the intermediate and slow time-scales as this corresponds to the steady-state flapping motion of the rotor. This would seem to be obvious since, in such a model, one is not interested in the free motion of the blade but how the blade motion is transmitted to the airframe. In accordance with this, the fast blade motions are usually neglected for piloted flight simulation, and the blade is assumed to respond instantaneously to control inputs, pitch motion and helicopter velocity. This is, in fact, an asymptotic approximation to the complete flapping behaviour and can be expressed in a first approximation as a truncated Fourier series:

$$\beta = a_0 - a_1 \cos\psi - b_1 \sin\psi \qquad (1)$$

where a_0, a_1 and b_1 are the so-called rotor-disc tilt angles representing respectively coning angle, longitudinal tilt and lateral tilt of the tip-path-plane (or no-feathering plane) and β is the blade flapping angle.

The rotor disc-tilt angles are usually expressed at different levels of approximation in the literature of speciality. Next paragraphs will identify two levels of calculating these angles: first, a simple formulation for the disc tilt attitude depending on first-order effects influencing blade flapping motion and second a more complicated formulation allowing for high-order coupling effects which can affect the blade flapping motion. Both formulations are derived using concepts originating from classical lifting line theory. In the case of a helicopter rotor blade, the validity of these models is questionable since its sections encounters unsteady and yawed flow. Therefore, the above assumption will be removed and formulae for the disc-tilt angles will be presented derived using a formulation of lifting line theory in which the effects of unsteady and swept flow are taken into account.

'Bramwell' rotor disc- tilt angles

One of the most simple and used formulae to express the attitude of the disc is presented in ref. [3]. Neglecting flapping hinge offset ($\varepsilon = 0$) and including in a first order the effects of helicopter roll rate p and pitch rate q, the rotor disc-tilt angles w.r.t. the no-feathering plane are [3]:

$$a_0 = \frac{\gamma}{8}\left[\theta_0\left(1+\mu_x{}^2\right)+\frac{4}{3}\lambda+\frac{2}{3}\mu_x\bar{p}\right]$$
$$a_1 = \frac{\frac{8}{3}\mu_x\theta_0+2\mu_x\lambda+\bar{p}-\frac{16}{\gamma}\bar{q}}{1-\mu_x{}^2/2} \qquad (2)$$
$$b_1 = \frac{4\mu_x a_0/3+\bar{q}-\frac{16}{\gamma}\bar{p}}{1+\mu_x{}^2/2}$$

These angles are derived assuming that the induced velocity is distributed uniform along the rotor disc. In order to account for the effects of non-uniform induced velocity distribution along the disc, a correction factor K is usually included in the formula of the lateral disc-tilt resulting in:

$$b_1 = \frac{4\mu_x a_0/3+\bar{q}-\frac{16}{\gamma}\bar{p}}{1+\mu_x{}^2/2}+\frac{K\lambda_0}{1+\mu_x{}^2/2} \qquad (3)$$

The correction factor K may be expressed as:

$$K = \frac{1.33\mu_x/|\lambda|}{1.2+\mu_x/|\lambda|} \qquad (4)$$

Effects of high-order coupling terms on the rotor disc-tilt angles

Retaining the high-order coupling terms in deducing the rotor disc-tilt angles, reference [11] obtained closed-form expressions for the rotor disc-tilt angles as expressed w.r.t. shaft plane. Transposing these relations to the no-feathering plane, one obtains:

$$\frac{\gamma}{8}\left[\frac{8}{\gamma}(1-2\bar{r})+\frac{4}{3}\theta_0\mu_x\bar{q}\right]a_0+\frac{\gamma}{8}\left[\begin{matrix}\theta_0\bar{p}+\frac{2}{3}\mu_x\bar{r}\\+\frac{2}{3}\lambda\bar{p}\end{matrix}\right]a_1+$$
$$\frac{\gamma}{8}\left[-\theta_0\bar{q}-\frac{2}{3}\mu_y\bar{r}-\frac{2}{3}\lambda\bar{q}\right]b_1=$$
$$=\frac{\gamma}{8}\left[\theta_0\left(1-2\bar{r}+{\mu_x}^2\right)\right]+\frac{\gamma}{8}\left[\frac{2}{3}\mu_x\bar{p}+\frac{2}{3}\mu_y\bar{q}+\frac{4}{3}\lambda\right]$$

$$\frac{\gamma}{8}\left[2\theta_0\bar{q}-\frac{4}{3}\mu_y-\frac{4}{3}\bar{h}_r\bar{p}+\frac{4}{3}\lambda\bar{q}\right]a_0+$$
$$+\frac{\gamma}{8}\left[1-\bar{r}-\frac{1}{2}{\mu_x}^2+\frac{1}{2}{\mu_y}^2+\mu_x\bar{h}_r\bar{q}+\mu_y\bar{h}_r\bar{p}\right]a_1+$$
$$\frac{\gamma}{8}\left[\frac{8}{\gamma}2\bar{r}-2\theta_0\mu_x\bar{q}+\mu_x\mu_y+\mu_x\bar{h}_r\bar{p}-\mu_y\bar{h}_r\bar{q}\right]b_1=$$
$$=\frac{\gamma}{8}\left[-\frac{16}{\gamma}\bar{q}+\frac{8}{3}\theta_0\left(\mu_x-\bar{h}_r\bar{q}\right)\right]+$$
$$\frac{\gamma}{8}\left[2\mu_x\mu_z-2\mu_x\lambda_0-2\bar{h}_r\bar{q}\lambda+\bar{p}\right] \qquad (5)$$

$$\frac{\gamma}{8}\left[-2\theta_0\bar{p}+\frac{4}{3}\mu_x(1-\bar{r})-\frac{4}{3}\bar{h}_r\bar{q}-\frac{4}{3}\lambda\bar{p}\right]a_0+$$
$$+\frac{\gamma}{8}\left[\begin{matrix}\frac{8}{\gamma}2\bar{r}+\theta_0\left(-\frac{2}{3}\mu_x\bar{q}+2\mu_y\bar{p}\right)-\mu_x\mu_y\\-\mu_x\bar{h}_r\bar{p}\end{matrix}\right]a_1+$$
$$\frac{\gamma}{8}\left[-1+\bar{r}-\frac{1}{2}{\mu_x}^2+\frac{1}{2}{\mu_y}^2+\mu_x\bar{h}_r\bar{q}\right]b_1=$$
$$=\frac{\gamma}{8}\left[\frac{16}{\gamma}\bar{p}+\frac{8}{3}\theta_0\left(\mu_y+\bar{h}_r\bar{q}\right)\right]+$$
$$\frac{\gamma}{8}\left[2\mu_y\mu_z-2\mu_y\lambda_0+2\bar{h}_r\bar{p}\lambda+\bar{q}\right]$$

Rotor disc-tilt angles with an improved sweep correction

In the usual flight-dynamics analyses of the helicopter rotor, models are used still originating from the simple concepts of the classical lifting-line theory. The validity of the models derived using these concepts is rather questionable, when thinking that this theory is strictly applicable for the analysis of high aspect ratio wings in steady flow and that the helicopter rotor blade is operating more in unsteady and yawed flow. Reference [4], questioning the validity of the simple sweep correction in relation to the lift, developed a special formulation of lifting-line theory, which takes the effects of unsteady and swept flow correctly into account. This theory leads to the conclusion that the effect of sweep may be equated to unsteady effects of the airfoil. Later, using the above formulation, reference [5] derived simple engineering corrections in order to account for the sweep effect on the attitude of the rotor's tip-path-plane and incorporated it into the usual formulation of the rotor disc-tilt angles for flight mechanics applications. Including the effects of both pitch and roll rates, the rotor disc-tilt formulae w.r.t. the control plane derived in ref. [5] were extended to the following expressions:

$$a_0=\frac{\gamma}{8}\left[\theta_0\left(1+{\mu_x}^2\right)+\frac{4}{3}\lambda+\frac{2}{3}\mu_x\bar{p}+\delta\left(\mu_x a_0-\frac{4}{3}b_1\right)\right]$$

$$a_1=\frac{2\mu_x\left(4\theta_0/3+\lambda\right)+\bar{p}-\frac{16}{\gamma}\bar{q}-\delta\mu_x b_1}{1-{\mu_x}^2/2} \qquad (6)$$

$$b_1=\frac{\frac{4}{3}\mu_x a_0+\bar{q}-\frac{16}{\gamma}\bar{p}+\delta\left(\frac{8}{3}\theta_0+2\lambda+\mu_x a_1\right)}{1+{\mu_x}^2/2}$$

where δ is the sweep correction factor given by:

$$\delta=\frac{4}{6}\frac{\mu_x\pi\sigma}{N}\ln\left(\frac{4}{3}\frac{\mu_x\pi\sigma}{N}\right) \qquad (7)$$

The next paragraph will analyse the effect of different approximations in the rotor-disc tilt angles, first in trim and then in manoeuvring flight. The following approximations for the rotor disc-tilt will be considered:

- the Bramwell's formulae (2);
- the effects of high-order coupling terms as given by (5);
- the effect of dynamic inflow correction factor K introduced in the lateral disc-tilt, formula (3)
- the effect of sweep correction factor δ;
- combination of K and δ effects.

5. Flight/Simulation Comparisons in Trimmed Flight

The effects of different disc-tilt approximations in the 6-dof piloted simulation model were first investigated for various trim conditions. As helicopter example, it was chosen for the hingeless Bo-105. Comparisons between DLR flight test data and simulations results as a function of airspeed up to 65 m/s (i.e. 234 km/h or advance ratio μ=0.3) are shown in Figs. 3 to 6 for the helicopter controls and Figs. 7 to 9 for the rotor disc-tilt angles.

Figure 3 illustrates the collective pitch in trim. One may observe an underprediction of about 38% over the whole speed range. The shortfall in hover is typical of this level of modelling, being attributed, as described in ref. [6], to the simplification made in accounting the fuselage download effects and the underprediction of the induced power by simple momentum theory. Similarly, the shortfall at high speed is consistent with a 40% underprediction in overall drag. All the different formulations in the disc-tilt angles are very closely as simulation results.

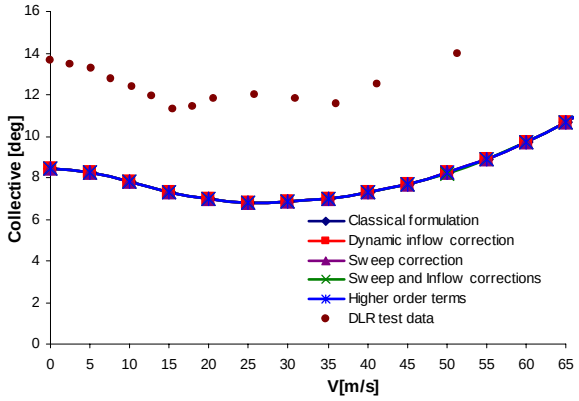

Fig. 3: Main rotor collective as a function of airspeed in trimmed flight

Concerning the longitudinal cyclic, Fig. 4 shows large discrepancies between the simulations and the flight test data (of about 80%). Cyclic is needed to balance the asymmetric flow together with fuselage and empennage pitching moments. The inclusion of a simple downwash for the horizontal stabiliser is responsible for about half of this discrepancy as pointed out in reference 6. Flight test results performed with Bo-105 in 1968 with a rigid rotor system showed a much higher lateral cyclic needed in trim (see Fig. 4 in which test data from reference [9] were used). Thus, the rotor system rigidity is another factor affecting the trim lateral cyclic. In this last case, the errors between the 6-dof simulation results and the flight data are decreasing to about 24% at high forward speeds.

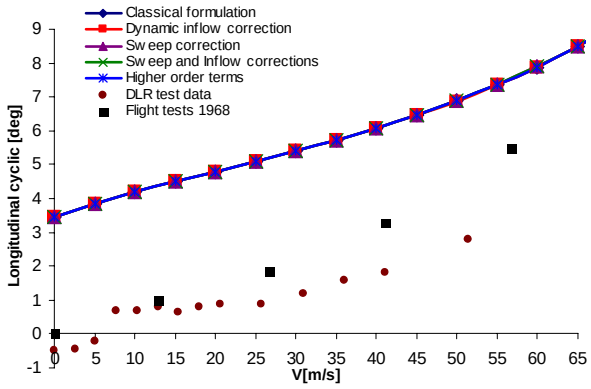

Fig.4: Longitudinal cyclic as a function of airspeed in trimmed flight

Fig. 5 shows the lateral cyclic pitch. It is interesting to comment here the differences obtained in the results when using different approximations for the rotor disc-tilt angles. The classical Bramwell formulation and the inclusion of the high-order coupling terms underpredict, as expected, enormously the flight test data (the high-order coupling terms are mainly in the helicopter angular rates which in trim are nil). Only sweep correction underpredicts the lateral cyclic at low velocities with about 71% (as related to the peak), the results improving at higher speeds. Including a simple dynamic inflow correction factor succeeds in catching the correct shape variation of the lateral cyclic as a function of sped. However, this correction alone still underpredicts with approximate 15% the peak lateral cyclic obtained at 15 m/s (54 km/h, μ=0.068) in the flight test but approximates very well the flight test data at high speeds. Accounting for both sweep and dynamic inflow corrections gives a 4% error in the peak lateral cyclic, thus both corrections applied to the model being able to account successfully for this peak at low forward speeds. Furthermore, at high speeds the sweep correction overpredicts the lateral cyclic with about 40%.

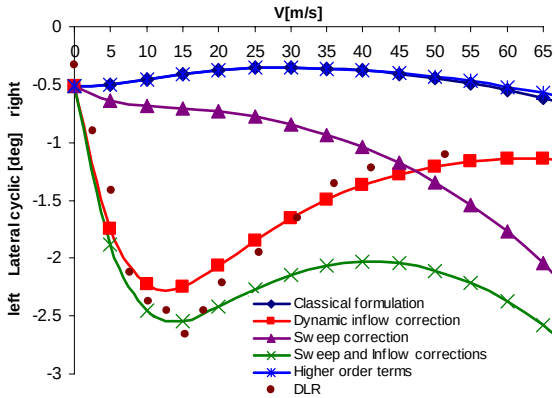

Fig. 5: Lateral cyclic as a function of airspeed in trimmed flight

It can be concluded that, whereas the sweep correction in combination with the dynamic inflow correction makes sure that the flight test peak in lateral cyclic is achieved, at high speeds the application of a sweep correction results in notable errors in the simulation model. Reference [6] reviewing the results of Garteur AG06 exercise comes to the conclusion that all state-of-the-art models up to date still fail to predict well the migration of left stick at low speed. The cause is attributed to the powerful effect of non-uniform inflow on rotor flapping and the corresponding cyclic pitch. At the moment, the best results are obtained with a model using a combination of the Pitt-Peters theory and empirical fitting of the coefficients in the longitudinal variation of the rotor inflow. The sweep correction introduced in the

present paper accounts for an extra effect, which was never accounted in the simulation models, namely the unsteady effects of an airfoil.

Referring to the pedal position, Fig. 6 shows that the flight test data are quite scattered. Hover pedal position is predicted within 9% by the present 6-dof simulation model.

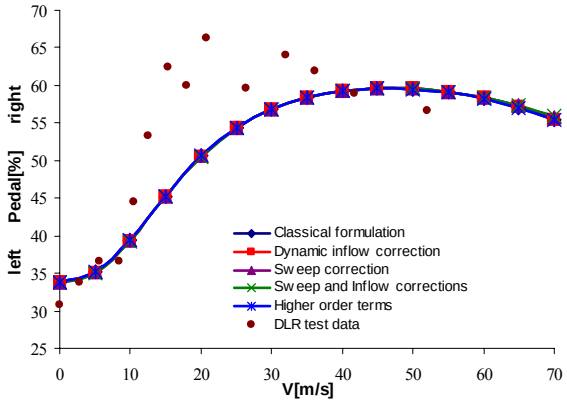

Fig.6: Pedal position as a function of airspeed in trimmed flight

Concerning the rotor disc-tilt angles, Fig. 7 to 10 shows the rotor disc-tilt attitude in trimmed flight in the 6-dof model.

Fig. 7 indicates that the coning angle is overpredicted with approximately 14 % over the whole speed range. A sweep correction results in an increasing of the trim coning angle of about 1.5% with respect to the classical formulae of Bramwell.

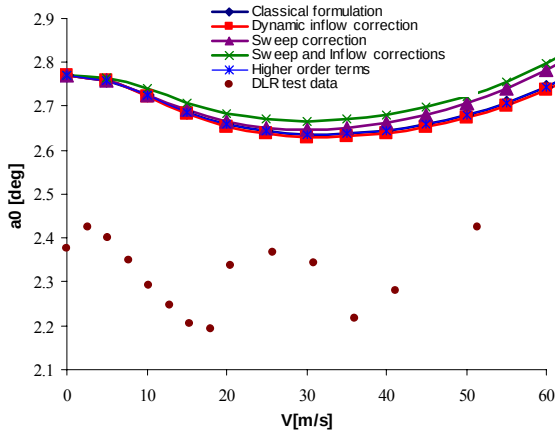

Fig.7: Coning angle as a function of airspeed in trimmed flight

Fig. 8 shows a favourable comparison for longitudinal disc-tilt angle over a wide speed range.

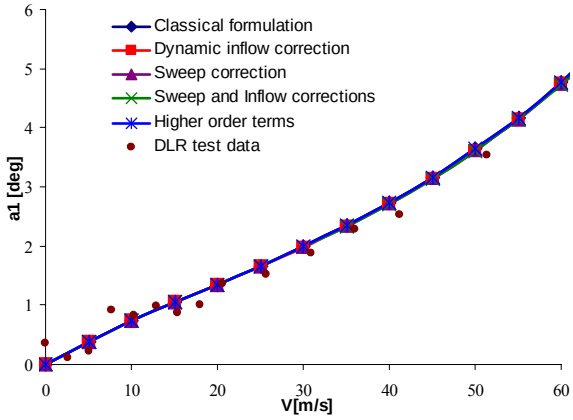

Fig. 8: Longitudinal rotor disc-tilt as a function of airspeed in trimmed flight

The lateral disc-tilt angle is illustrated in Fig. 9 and can be close correlated to the results and interpretation given to the lateral cyclic (see Fig. 5). In this respect, one may observe that including both a sweep and a dynamic inflow correction results in predicting the peak lateral disc-tilt reached at about 15 m/s (μ=0.068) during flight tests. However, a sweep correction introduces large discrepancies at high speeds between the model and the flight test data.

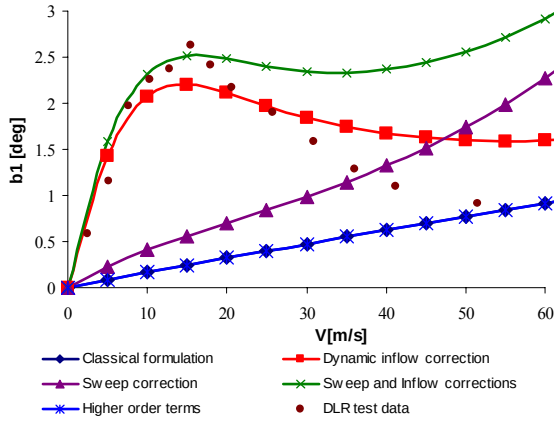

Fig. 9: Lateral rotor disc-tilt as a function of airspeed in trimmed flight

6. Flying Longitudinal and Lateral Doublets

It was decided to get first a feeling of the rotor disc-tilt effects during manoeuvring flight by flying initially doublets given in longitudinal and lateral cyclic. Fig. 12 presents the attitude rate responses when performing a doublet in longitudinal cyclic.

Once more, different approximations in the rotor disc-tilt angles are assumed. The striking difference in these graphs is to be seen mainly in the off-axis responses (see lateral cyclic stick or body lateral

velocity v) and is due to the dynamic inflow modelling.

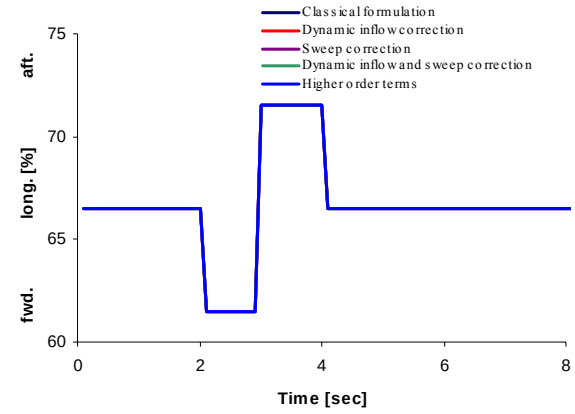

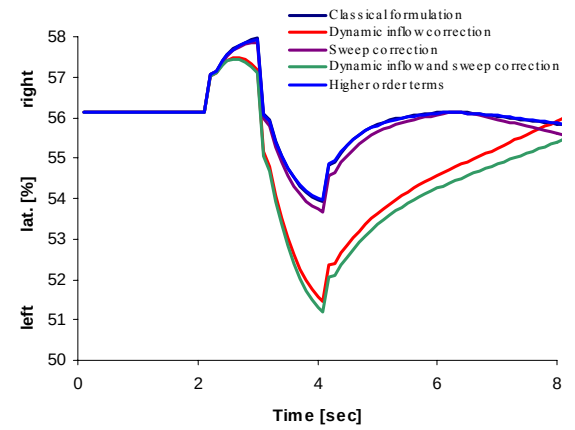

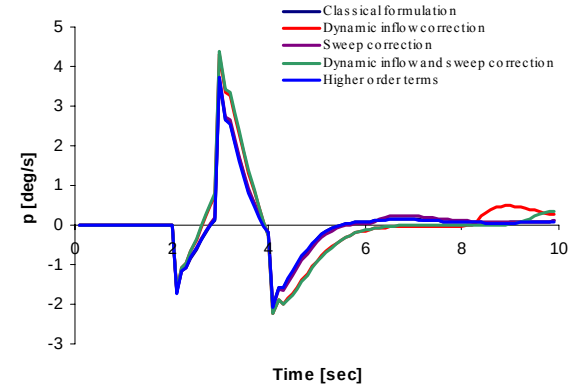

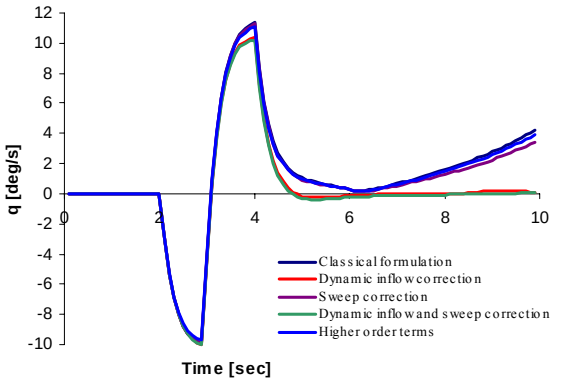

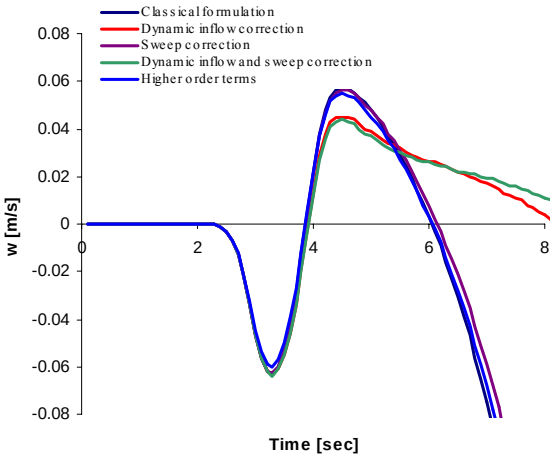

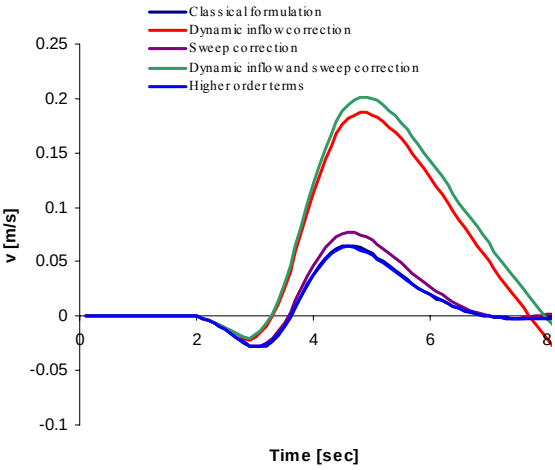

Fig. 12: Flying a doublet in longitudinal cyclic

From Fig. 12 it can be seen that including a correction factor in the dynamic inflow results in: 1% more pilot lateral cyclic stick to the right and 5% more to the left w.r.t. the classical formulation; 75% more body lateral velocity. The body vertical velocity is increasing with about 33% compared to the classical formulation. Some differences in pedal and yaw rate were also observed: in the classical disc-tilt formulation, the pilot applies the pedal to the right whereas when using dynamic inflow correction the pilot applies the pedal to the left). The effect of high-order coupling terms in performing the longitudinal doublet is negligible. In addition, including only sweep correction in the model does not affect the simulation results. Reference [6], assessing the effects of different dynamic inflow models on the helicopter response characteristics, concluded that using a more complex model for dynamic inflow during pitching manoeuvres results in 'striking' improvements in the simulation results. This is due to the fact that during longitudinal manoeuvres, the strong perturbations in normal velocity w induce an inflow response in the laterally distributed aerodynamic loads on the rotor.

Figure 13 plotted the rotor disc-tilt angles during the longitudinal cyclic doublet. From this figure it can be red an increasing of 60% in the lateral tilt of the rotor disc w.r.t. the classical formulation when the dynamic inflow correction is introduced in the model.

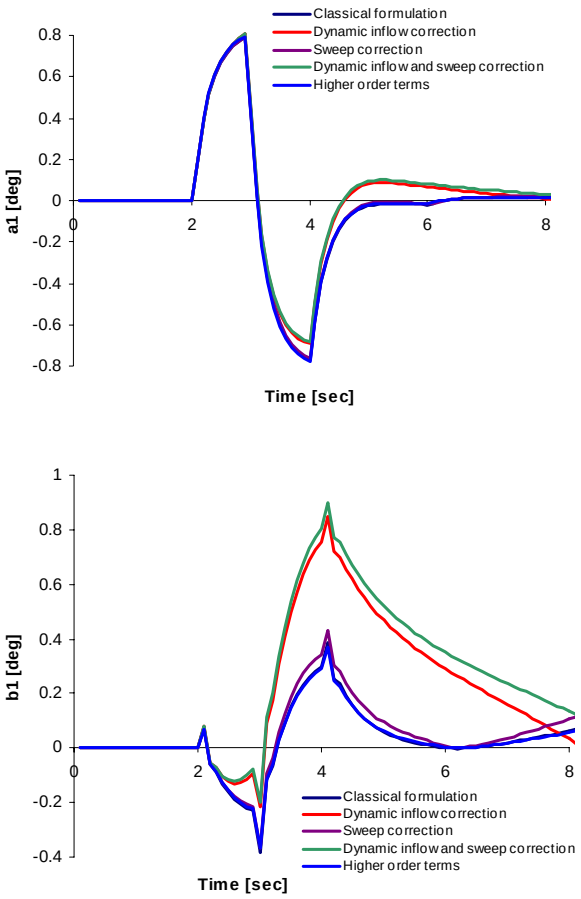

Fig. 13 Response in Rotor disc-tilt angles to longitudinal doublet

In contrast, the effects of dynamic inflow on the roll axis are hardly remarkable.

Figure 14 illustrates the helicopter response to a doublet in lateral cyclic. First of all, it should be mentioned that it was very difficult to fly this manoeuvre using the pilot model of the 6-dof model. The roll to pitch coupling is in this case the critical factor in the simulations. This can be seen also in Fig. 14 on the results obtained when using high-order coupling terms in the rotor disc-tilt formulae.

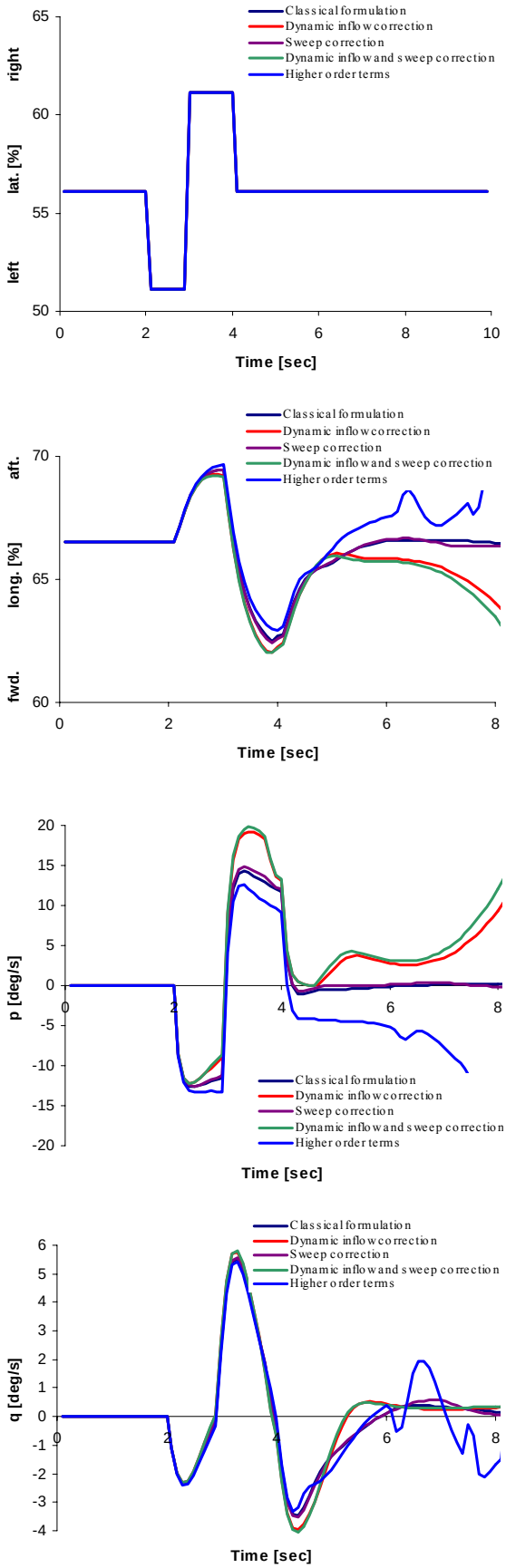

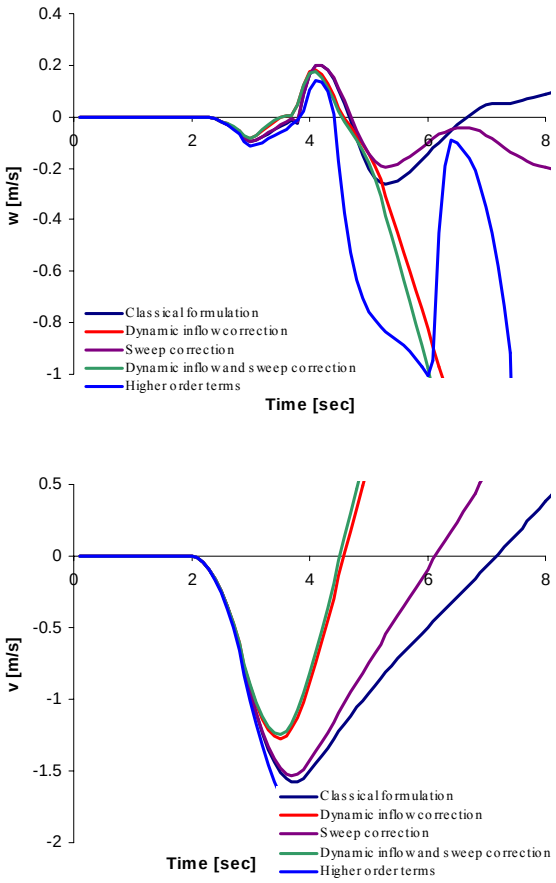

Fig. 14: Flying a doublet in lateral cyclic

This off-axis response deficiency in a rolling manoeuvre is a well-known problem and has been the subject of several studies. Some of the solutions proposed refer to a better wake modelling. The present results indicate that a better approximation in the rotor disc tilt angles by inclusion of high-order coupling terms in pitch, roll and yaw rates improve as well the simulation results. Figure 15 shows the disc-tilt angles during a lateral doublet.

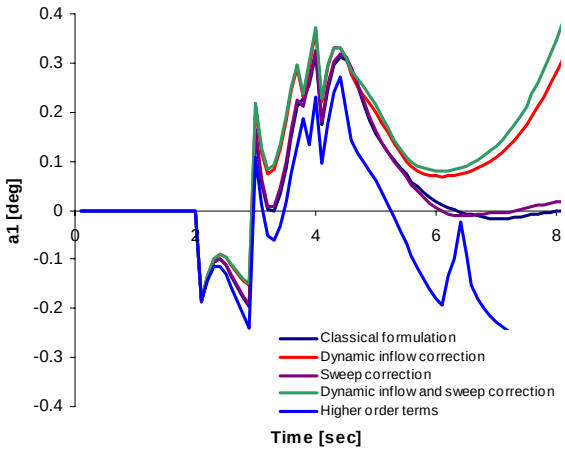

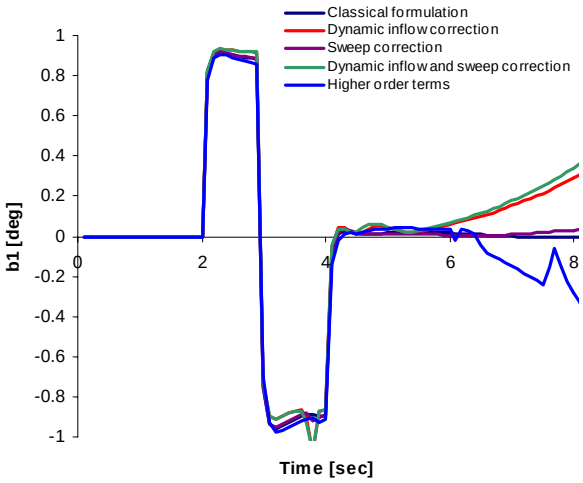

Fig. 15 Response in Rotor disc-tilt angles to lateral doublet

It can be seen that inclusion of high-order coupling terms in the disc-tilt formulae affect the longitudinal disc-tilt.

7. Flying the Acceleration/Deceleration Manoeuvre

One of the most common manoeuvres of the ADS-33 [ref. 2] defined in order to assess the performance and agility of the rotorcraft in the longitudinal plane is the acceleration/deceleration manoeuvre.

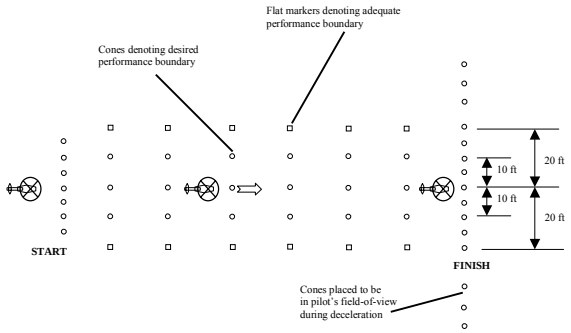

Fig. 16 Acceleration/Deceleration manoeuvre

The manoeuvre is described as follows in the ADS-33 (see Fig. 16): "*Start from a stabilized hover. In a good vision environment, rapidly increase power to approximately maximum, maintain altitude, constant with pitch attitude, and hold collective constant during the acceleration to airspeed of 50 knots (approximately 26m/s). Upon reaching the target airspeed, initiate a deceleration by aggressively reducing the power and holding altitude constant with pitch attitude. The peak nose-up attitude should occur just before reaching the final stabilized hover.*"

The manoeuvre was performed in the 6-dof piloted model following four stages:

- Stage 1 Hover: maintain for a short period (approx. 1.5 sec) a clean hover (i.e. constant control inputs);
- Stage 2 Accelerating: achieve acceleration up to the target airspeed, which is 50 knots (approximately 26m/s). This is done by using forwards movement of the longitudinal cyclic and by reason of altitude hold condition increasing the collective;
- Stage 3 Decelerating first from 50 to 25 knots. Two control inputs were used, i.e. backwards movement of longitudinal cyclic and by reason of altitude hold condition decreasing in the collective
- Stage 4 Continuing deceleration from 25 knots (approximately 13m/s) down to hover speed. This was achieved by moving the longitudinal cyclic forwards together with increasing the collective;
- Stage 5 Hover: maintain a stabilized hover for 5 seconds to complete the manoeuvre. Analogous to stage 1, this manoeuvre requires constant control inputs.

The acceleration/deceleration manoeuvre was flown in the 6-dof model using different approximations for the rotor disc-tilt angles.

Fig. 17 illustrates the pilot controls during acceleration/deceleration using different approximations in the rotor disc-tilt angles. The effect of different approximations is caught in the pilot lateral cyclic stick. Using the dynamic inflow correction resulted in use of the left cyclic control in stage 4. The effect of high-order coupling terms in the model is important when performing this manoeuvre. The amplitude of the longitudinal cyclic changes slightly during the whole manoeuvre when using different approximations in the rotor disc-tilt. A maximum load factor of about 1.8 is achieved during acceleration, followed during deceleration by a decrease of more than 80% from this maximum value.

As concerning the helicopter responses during the acceleration/deceleration manoeuvre, Fig. 18 illustrates the importance of different disc-tilt models in calculating the lateral disc-tilt angle b_1. Using dynamic inflow correction results in an increasing with 75% of the lateral disc-tilt during the deceleration w.r.t. the classical formulation. High-order coupling terms reduce the lateral disc-tilt with about 50% w.r.t. the classical formulation. Sweep correction result in an increasing with 50% in the lateral disc tilt.

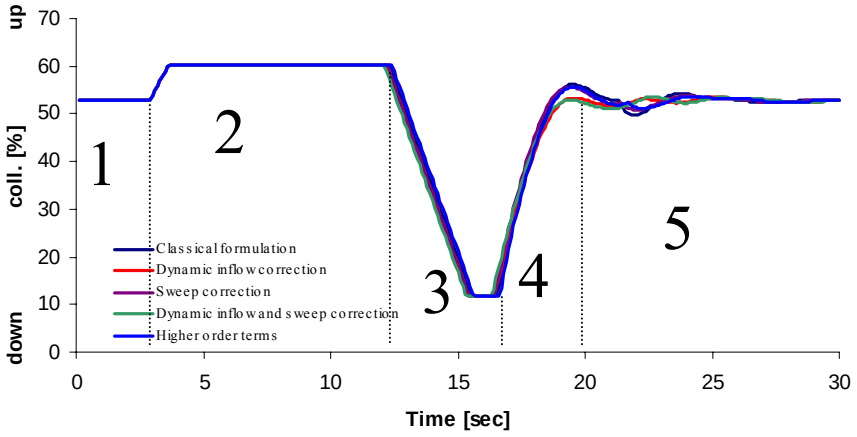

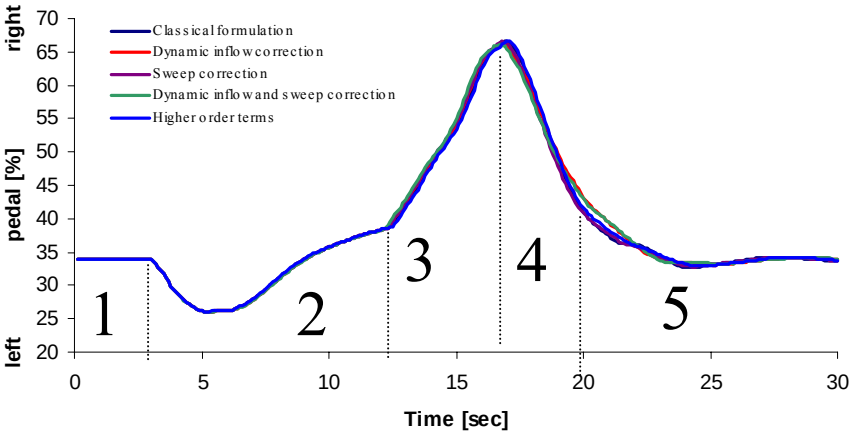

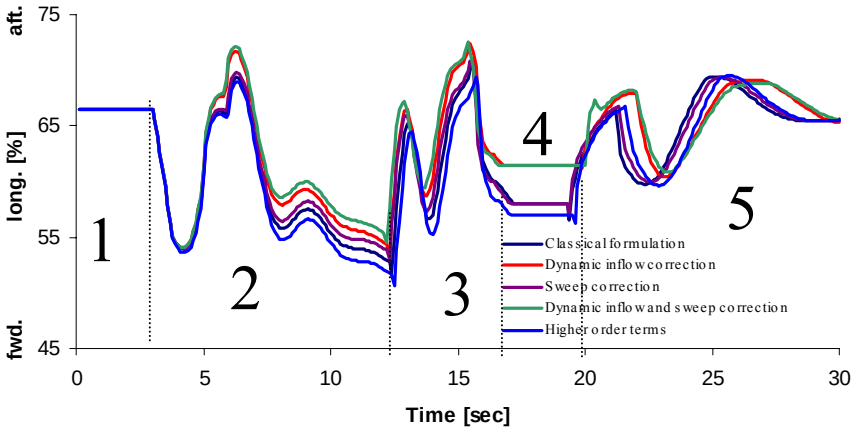

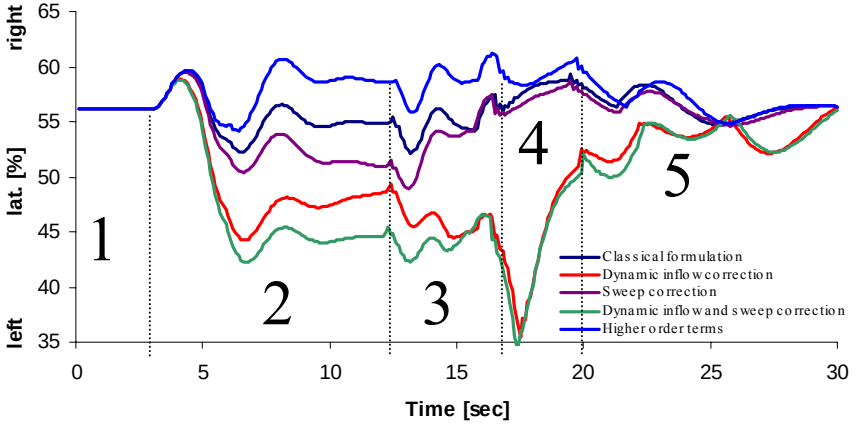

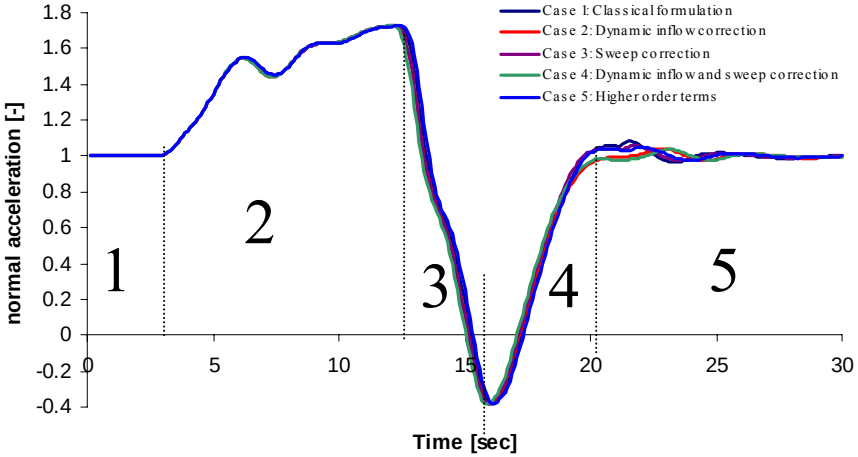

Fig. 17 Pilot controls and normal acceleration during accel/decel manoeuvre

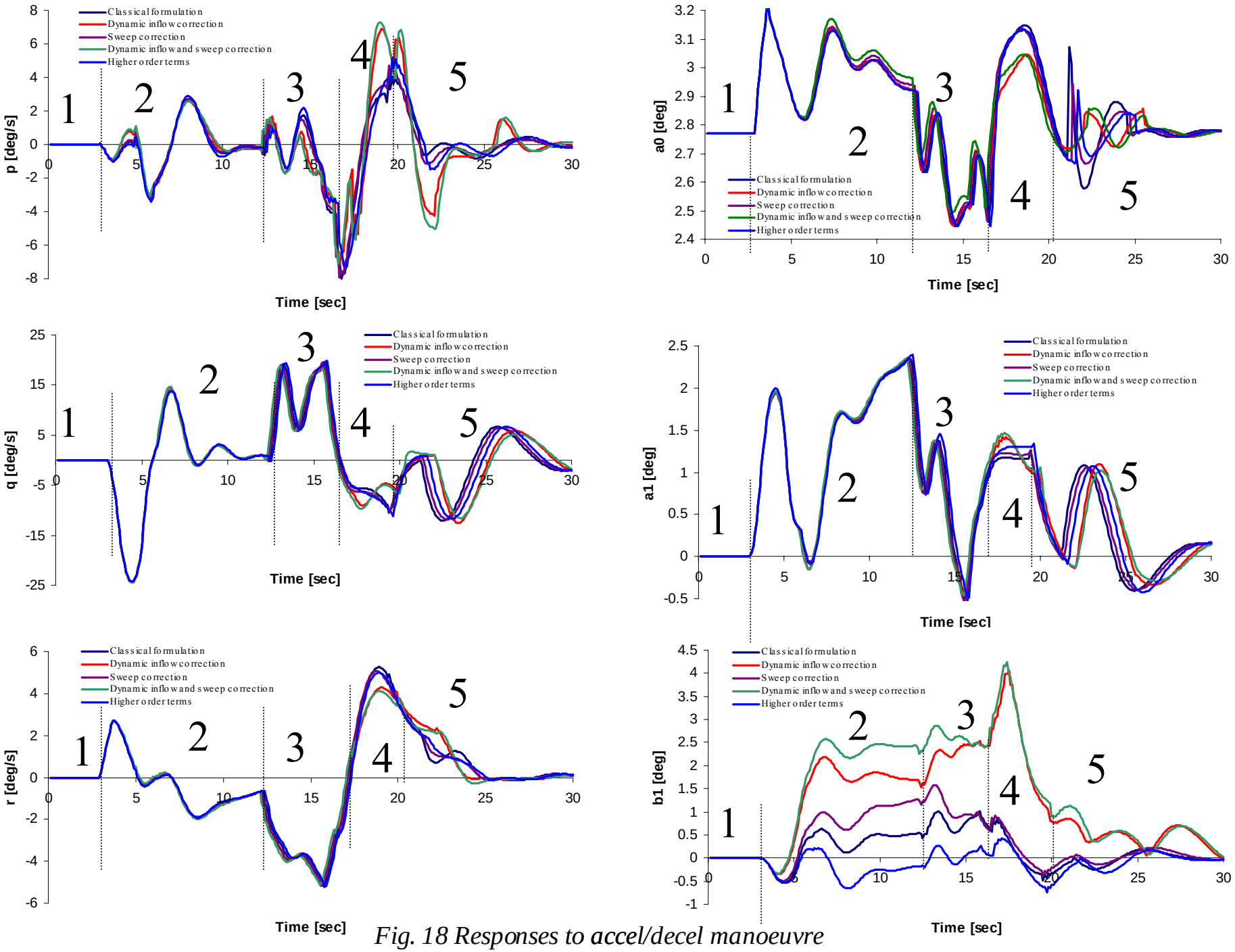

Fig. 18 Responses to accel/decel manoeuvre

8. Conclusions

The present paper presented the effects of different approximations made in expressing analytically the rotor disc-tilt angles on the helicopter trimmed and manoeuvring flight. The paper concentrated on the following disc-tilt approximations:

- a classical formulation as usually seen in the helicopter books;
- formulae including a dynamic inflow correction factor in the lateral disc-tilt angle accounting for the effects of non-uniform induced velocity distribution along the rotor disc;
- formulae including a sweep correction factor in the disc-tilt angles accounting for the effects of non-steady flow around the airfoil;
- formulae including both sweep and a dynamic inflow correction factors;
- formulae accounting for the high-order coupling terms in pitch, roll and yaw attitude rates;

The paper presented trim and time-domain simulations performed with a 6-dof non-linear piloted simulation model for the Bo-105 helicopter in which the rotor disc tilt angles approximations were varied.

With respect to the trim calculations of the Bo-105 in hover and different forward flight conditions, it appeared that considering a sweep correction factor together with a dynamic inflow correction factor resulted in only a 4% underprediction of the peak lateral tilt of the rotor disc in the flight region around $\mu = 0.1$. No up to the present models could account for this peak, most of the literature models resulting in errors of 30% to 40% even after the inclusion of a proper dynamic inflow model. This result indicates that including the sweep effect in the simulation model might give the solution for fully accounting the experimentally observed peak at low flight velocities. However, using both sweep and dynamic inflow corrections resulted in overpredicting the lateral disc-tilt for trimming at high flight speeds. The effects of high-order coupling terms in the disc-tilt formulae give no differences w.r.t. the classical formulation (this result was expected as these terms are coming mainly from the helicopter attitude rates which are zero in the trim).

With respect to the time-domain simulations, performing three manoeuvres (one doublet in longitudinal cyclic, one doublet in lateral cyclic and the acceleration/deceleration manoeuvre from the ADS-33 standard) led to the following conclusions:

- dynamic inflow correction factor in the lateral disc-tilt is important in a pitch axis manoeuvre;
- high-order coupling terms considered in the formulae of the disc-tilt angles are important in a roll axis manoeuvre;
- in acceleration/deceleration manoeuvre, the combination of all the correction factors (dynamic inflow, sweep and high-order coupling terms) is important, each of these parameters changing the predicted lateral disc-tilt angle.

Acknowledgements

Sincere thanks are due to Mr. Wolfgang von Grünhagen and Mr. Mario Hamers of DLR Braunschweig, Germany for providing test data of the Bo-105 and to Mr. Jasper van der Vorst of NLR Amsterdam, Netherlands for providing simulation results of Flightlab.

References

1. Aalst, Richard, van, "On the Question of Adequate Modelling of Steady-State Rotor Disc-Tilt for Helicopter Manoeuvring Flight, Draft Final Thesis Report, June 2002, Faculty of Aerospace Engineering, Delft University of Technology
2. anon., "Aeronautical Design Standard-33E PRF, Performance specification, Handling Qualities Requirements for Military Rotorcraft", US Army AMCOM, Redstone, Alabama, March, 2000
3. Bramwell, A.R.S., "Helicopter Dynamics", Edward Arnold (Publishers) Ltd, 1976
4. Holten, Th. van, "On the Validity of Lifting Line Concepts in Rotor Analysis", Vertica, vol.1, pp. 239-254, 1977
5. Holten, Th. van, "Upgrading of Classical Lifting-Line Theory to Obtain Accurate Flight Mechanical Helicopter models: Improved Correction for Sweep Effects" AGARD-FVP Symposium "Advances in Rotorcraft Technology", 27-30 May 1996, Ottawa, Canada
6. Padfield, G.D., et.al., "Predicting Rotorcraft Flying Qualities through Simulation Modelling. A Review of Key Results from Garteur AG06", 22nd European Rotorcraft Forum, 15-17 September, 1996, Brighton, United Kingdom, paper no. 71
7. Pavel, M. D., "Effects of Rotor Disc-Tilt on Helicopter Piloted Simulation", 24th European Rotorcraft Forum, 15-17 September, 1998, Marseilles, France, paper no. FM 03
8. Pavel, Marilena D., "On the Necessary Degrees of Freedom for Helicopter and Wind Turbine Low-Frequency Mode-Modelling", Ph.D.

Dissertation, Delft University of Technology, 2001
9. Reichert, G., and Oelker, P., "Handling Qualities with the Bolkow Rigid Rotor System", 24th Annual National Forum, American Helicopter Society, Washington DC, May 1968, preprint 218
10. Vorst, J. van der, and Stegeman, J.D., "A Pilot Model for Helicopter Maneuvres", 24th European Rotorcraft Forum, 15-17 September, 1998, Marseilles, France
11. Ypma, F.A.K., "On the Prediction of Blade Flapping Angles", M-730, TU Delft, Dec. 1996

Appendix A

Derivation of the equations of motion in a six degree-of-freedom model

In a general 6-dof non-linear body model the helicopter motion is represented by three translations and three rotations around the body axes-system $\overline{E}_b\{x\ y\ z\}$ centred in the helicopter centre of gravity O and with z axis parallel with the rotor axis. System $\overline{E}_0\{x_0\ y_0\ z_0\}$ is centred in the helicopter's centre of gravity and has the axes parallel with the inertial system $\overline{E}_E\{x_E\ y_E\ z_E\}$. The orientation of the three axes system is given in figure A1.

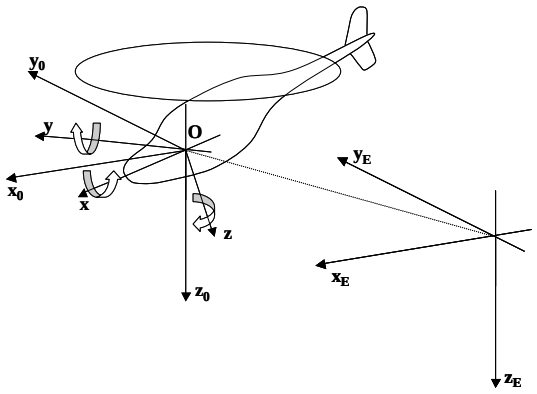

Fig. A1: System of coordinated used to express the motion of the helicopter in the 6-dof model

Using the assumptions described in paragraph "Six Degree-of-Freedom for Piloted Simulation" of the paper, the helicopter equations of motion in the body axes system are derived starting from the fundamental equations of dynamics in the matrical form:

$$\begin{cases} \dfrac{d}{dt}\{H\} = [m]\{a\} = [m]\{\dot{V}\} + [m][\omega_x]\{V\} = \{F\} \\ \dfrac{d}{dt}\{K\} = [J]\{\dot{\Omega}\} + [\omega_x][J]\{\Omega\} = \{M_0\} \end{cases} \quad \text{(A1)}$$

wherein, for the helicopter:

$\{H\} = \{H_x H_y H_z\}^T$ vector of impulses

$\{K\} = \{K_x K_y K_z\}^T$ vector of moment impulses

$[m] = \begin{bmatrix} m & 0 & 0 \\ 0 & m & 0 \\ 0 & 0 & m \end{bmatrix}$ matrix of mass

$\{a\} = \{a_x a_y a_z\}^T$ vector of accelerations

$\{\dot{V}\} = \{\dot{u}\ \dot{v}\ \dot{w}\}^T$ vector of linear accelerations

$\{V\} = \{u\ v\ w\}^T$ vector of linear velocities

$\{F\} = \{F_x F_y F_z\}^T$ vector of forces

$\{\Omega\} = \{p\ q\ r\}^T$ vector of angular velocities

$\{\dot{\Omega}\} = \{\dot{p}\ \dot{q}\ \dot{r}\}^T$ vector of angular accelerations

$[\omega_x] = \begin{bmatrix} 0 & r & -q \\ -r & 0 & p \\ q & -p & 0 \end{bmatrix}$ matrix of rotation

$[J] = \begin{bmatrix} I_x & 0 & -I_{xz} \\ 0 & I_y & 0 \\ -I_{xz} & 0 & I_z \end{bmatrix}$ moment of inertia matrix

$\{M_0\} = \{L\ M\ N\}^T$ vector of moments w.r.t. the helicopter centre of gravity

Taking into account the fact that $\overline{E}_b$ relates to $\overline{E}_0$ by Euler angles $\{\phi,\theta,\psi\}$) and that the total components of forces and the moments on the helicopter body is a summation of the corresponding components on each helicopter component, after expanding, one obtains the helicopter equations of motion in the system $\overline{E}_0$ expressed as:

$$\begin{aligned} \dot{u} &= \frac{X_{Weight}}{m} + \frac{X_{MR}}{m} + \frac{X_{FUS}}{m} - \frac{D \cdot u}{m \cdot v} + rv - qw \\ \dot{v} &= \frac{Y_{Weight}}{m} + \frac{Y_{MR}}{m} + \frac{Y_{TR}}{m} + \frac{Y_{FIN}}{m} - ru + pw \\ \dot{w} &= \frac{Z_{Weight}}{m} + \frac{Z_{MR}}{m} + \frac{Z_{FUS}}{m} + \frac{Z_{HS}}{m} + \frac{D \cdot w}{m \cdot v} - pv + qu \\ \dot{p} &= \frac{L_{MR} + L_{TR} + L_{FIN} - (I_x - I_y)qr + (\dot{r} + pq)I_{xz}}{I_x} \\ \dot{q} &= \frac{M_{MR} + M_{FUS} + M_{HS} - (I_x - I_y)pr + (p^2 - r^2)I_{xz}}{I_y} \\ \dot{r} &= \frac{N_{MR} + N_{TR} + N_{FIN} - (I_y - I_x)pq + (\dot{p} - rq)I_{xz}}{I_z} \end{aligned} \quad \text{(A2)}$$

$$\dot{\phi} = p + \dot{\psi}\sin\theta$$
$$\dot{\theta} = q\cos\phi - r\sin\phi \qquad \text{(A3)}$$
$$\dot{\psi} = q\frac{\sin\phi}{\cos\theta} + r\frac{\cos\phi}{\cos\theta}$$

In order to describe completely the helicopter motion w.r.t. the Earth system $\overline{E}_E$, the equations of trajectory can be added:

$$\dot{x} = (u\cos\theta + (v\sin\phi + w\cos\phi)\sin\theta)\cos\phi$$
$$-(v\cos\phi - w\sin\phi)\sin\phi$$

$$\dot{y} = (u\cos\theta + (v\sin\phi + w\cos\phi)\sin\theta)\sin\phi \qquad \text{(A4)}$$
$$-(v\cos\phi - w\sin\phi)\cos\phi$$

$$\dot{z} = (u\sin\theta - (v\sin\phi + w\cos\phi))\cos\theta$$

The system of equations (A3)+(A4) describe completely the motion of the helicopter in an inertial system. To these systems of equations, two differential equations are added for the dynamic inflow of the main and tail rotor, describing the dynamic inflow as a "quasi-steady inflow" by means of the time constants:

$$\tau_{\lambda_0}\dot{\lambda}_0 = C_{T,Elem} - C_{T,Glauert} \qquad \text{(A5)}$$
$$\tau_{\lambda\ tr}\dot{\lambda}_{tr} = C_{T,Elem\ tr} - C_{T,Glauert\ tr}$$

The forces and moments exerted on each helicopter component are illustrated in Fig. A2 and will be further analytical expressed.

The projection of the gravity force on the inertial system is:

$$X_{Weight} = -mg\sin\theta$$
$$Y_{Weight} = mg\cos\theta\sin\phi \qquad \text{(A6)}$$
$$Z_{Weight} = mg\cos\phi\cos\theta$$

The total forces and moments on the main rotor are:

$$X_{MR} = -\frac{T_D}{m}\sin(a_1 - \theta_{1s})\cdot\cos(b_1 + \theta_{1c})$$
$$-\frac{H_D}{m}\cos(a_1 - \theta_{1s}) + \frac{S_D}{m}\sin(a_1 - \theta_{1s})\cdot\sin(b_1 + \theta_{1c})$$
$$Y_{MR} = \frac{T_D}{m}\sin(b_1 + \theta_{1c}) + \frac{S_D}{m}\cos(b_1 + \theta_{1c})$$
$$Z_{MR} = -\frac{T_D}{m}\cos(a_1 - \theta_{1s})\cdot\cos(b_1 + \theta_{1c})$$
$$+\frac{H_D}{m}\sin(a_1 - \theta_{1s}) + \frac{S_D}{m}\cos(a_1 - \theta_{1s})\cdot\sin(b_1 + \theta_{1c}) \qquad \text{(A7)}$$

$$L_{MR} = Y_{MR}\cdot z_h - Z_{MR}\cdot y_h + L_e$$
$$M_{MR} = -X_{MR}\cdot z_h - Z_{MR}\cdot x_h + M_e$$
$$N_{MR} = Q + X_{MR}\cdot y_h - Y_{MR}\cdot x_h$$

with L_e and M_e the moments on the hub resulting from the hinge offset of the rotor blades:

$$L_e = (\Omega R)_{MR}^2\,\varepsilon\cdot m_{bl}\sin(b_1 + \theta_{1c})$$
$$M_e = (\Omega R)_{MR}^2\,\varepsilon\cdot m_{bl}\sin(a_1 - \theta_{1s}) \qquad \text{(A8)}$$

The main rotor thrust T_D, horizontal force H_D (equivalent to a drag force), lateral force S_D and the main rotor torque are expressed by their non-dimensional coefficients as:

$$T_D = \rho(\Omega R)^2(\pi R^2)C_{tD}$$
$$H_D = \rho(\Omega R)^2(\pi R^2)C_{HD}$$
$$S_D = \rho(\Omega R)^2(\pi R^2)C_{SD} \qquad \text{(A9)}$$
$$Q_D = \rho(\Omega R)^2(\pi R^2)RC_{QD}$$

wherein, the non-dimensional coefficients are given by:

$$C_{TD} \approx C_{T,elem} = \frac{\sigma C_l^\alpha}{2}\left[\frac{\theta_0}{3}\left(1 + \frac{3}{2}\mu_x\right) + \frac{\mu_z - \lambda_0}{2}\right] \qquad \text{(A10)}$$

$$C_{SD} = C_S - C_T b_1 \qquad \text{(A11)}$$

$$C_S = \frac{\sigma C_l^\alpha}{2}\left[\mu_x^{\,2}\left(\frac{b_1\theta_0}{2} - a_0 a_1\right) + \mu_x\left(\frac{a_1 b_1}{4} + \frac{3\lambda a_0}{2} - \frac{3a_0\theta_0}{4}\right)\right.$$
$$\left. + \frac{\theta_0 b_1}{3} - \frac{3\lambda b_1}{4} + \frac{a_0 a_1}{6}\right] \qquad \text{(A12)}$$

$$C_{QD} = \frac{\sigma\ C_d}{8}\left(1 + 4.7\mu_x^{\,2}\right) + C_T\lambda_D - \mu_x C_{HD} \qquad \text{(A13)}$$

The main rotor thrust coefficient expressed with the Glauert equation is:

$$C_{T,Glauert} = 2\lambda_0\sqrt{\mu_x^{\,2} + (\mu_z - \lambda_0)^2)} \qquad \text{(A14)}$$

The fuselage participates to the motion by:

$$X_{FUS} = -R_{FUS}\cos(\alpha_{FUS})$$
$$Z_{FUS} = -R_{FUS}\sin(\alpha_{FUS}) \qquad \text{(A15)}$$

$$M_{FUS} = \rho V^2 K_{FUS} Vol_{FUS} \alpha_{FUS}$$

wherein the aerodynamic force on the fuselage is calculated through an equivalent drag area F_0:

$$R_{FUS} = \frac{1}{2}\rho V^2 F_0 \tag{A16}$$

Next, the horizontal and the vertical stabilizer are given by their forces and moments:

$$\begin{aligned} Z_{HS} &= -\frac{1}{2}\rho {V_{HS}}^2 \cdot 0.65 C_{l_\alpha HS} \alpha_{HS} \\ M_{HS} &= Z_{HS} \cdot x_{HS} \end{aligned} \tag{A17}$$

$$\begin{aligned} Y_{FIN} &= -\frac{1}{2}\rho {V_{FIN}}^2 S_{FIN} C_{l_\alpha, FIN} \beta_{FIN} \\ L_{FIN} &= -z_{FIN} \cdot Y_{FIN} \\ N_{FIN} &= -x_{FIN} \cdot Y_{FIN} \end{aligned} \tag{A18}$$

with the horizontal stabilizer local angle of attack:

$$\alpha_{HS} = \alpha_{0,HS} + \arctan\left(\frac{w + q \cdot x_{HS}}{u}\right) \tag{A19}$$

and velocity:

$${V_{HS}}^2 = u^2 + (w + q \cdot x_{HS})^2 \tag{A20}$$

The angle of attack of the fin is:

$$\beta_{FIN} = \beta_{0,FIN} + \arctan\left(\frac{v - r \cdot x_{FIN} - p \cdot z_{FIN}}{u}\right) \tag{A21}$$

and the local velocity:

$${V_{FIN}}^2 = u^2 + \left(v - r \cdot x_{FIN} - p \cdot z_{FIN}\right)^2 \tag{A22}$$

The tailrotor forces and moments on the helicopter are:

$$\begin{aligned} Y_{TR} &= T_{TR} \cdot F_{TR} \\ L_{TR} &= -Y_{TR} \cdot z_{TR} \\ N_{TR} &= -Y_{TR} \cdot x_{TR} \end{aligned} \tag{A23}$$

The tailrotor is modelled as an actuator disc with the tail rotor thrust given by:

$$T_{TR} = C_{T,elem,TR} \cdot \rho \left(\Omega R\right)_{TR}^2 \pi R_{TR}^2 \tag{A24}$$

$$C_{T_{elem},TR} = \frac{\sigma_{TR} C_{l,TR}^{\alpha}}{2}\left[\frac{\theta_{0,TR}}{3}\left(1 + \frac{3}{2}\mu_{x,TR}\right) + \frac{\left(\mu_{Z,TR} - \lambda_{0,TR}\right)}{2}\right] \tag{A25}$$

A fin blockage factor has been applied to the tail rotor side force as:

$$F_{TR} = 1 - \frac{3 \cdot S_{FIN}}{4\pi R_{TR}^2} \tag{A26}$$

Pilot model

Flying a rotorcraft with a 6-dof model a Stability Augmentation System (SAS) has to be implemented. For the manoeuvres used in this work, four stabilization functions are developed, each one for each helicopter control. The stabilization functions are PID (Proportional+Integral+Derivative) controllers [8, 10]:

Collective control

The collective stick controls vertical speed:

$$Collective = K_{vs}\left(vs_{req} - vs\right) + K_{\text{int}\_vs}\int\left(vs_{req} - vs\right)dt \tag{A27}$$

The required vertical speed is controlled by an "altitude hold" controller, feeding back the height to the vertical speed:

$$vs_{req} = K_h\left(h_{req} - h\right) \tag{A28}$$

Longitudinal cyclic control

The Longitudinal cyclic controls pitch attitude:

$$Longitudinal = K_\theta\left(\theta_{req} - \theta\right) + K_{\text{int}\_\theta}\int\left(\theta_{req} - \theta\right)dt + K_q q \tag{A29}$$

The required pitch attitude is controlled by a "longitudinal position hold" controller:

$$\theta_{req} = K_x\left(x_{req} - x\right) + K_{\text{int}\_x}\int\left(x_{req} - x\right)dt + K_{xdot}\dot{x} \tag{A30}$$

The required pitch attitude is also used as an "altitude hold" controller. In the 6-dof simulation pilot model two gain settings were used, an aggressive and a normal one:

$$\theta_{req} = K_{h1}\left(h_{req} - h\right) + K_{\text{int}\_h}\int\left(h_{req} - h\right)dt + K_{hdot}\dot{h} \tag{A31}$$

Lateral cyclic control

The Lateral cyclic stick controls roll attitude:

$$Lateral = K_\phi\left(\phi_{req} - \phi\right) + K_{\text{int}\_\phi}\int\left(\phi_{req} - \phi\right)dt + K_p p \tag{A32}$$

The required roll angle is controlled by a “lateral position hold” controller:

$$\phi_{req} = K_y \left(y_{req} - y \right) + K_{\text{int\_}y} \int \left(y_{req} - y \right) dt + K_{ydot} \dot{y} \tag{A33}$$

Pedal control

The pedals controls heading angle:

$$Pedal = K_\psi \left(\psi_{req} - \psi \right) + K_{\text{int\_}\psi} \int \left(\psi_{req} - \psi \right) dt + K_r r \tag{A34}$$

The required yaw angle is controlled fast and smooth and does not need any PID controller for the required yaw angle.

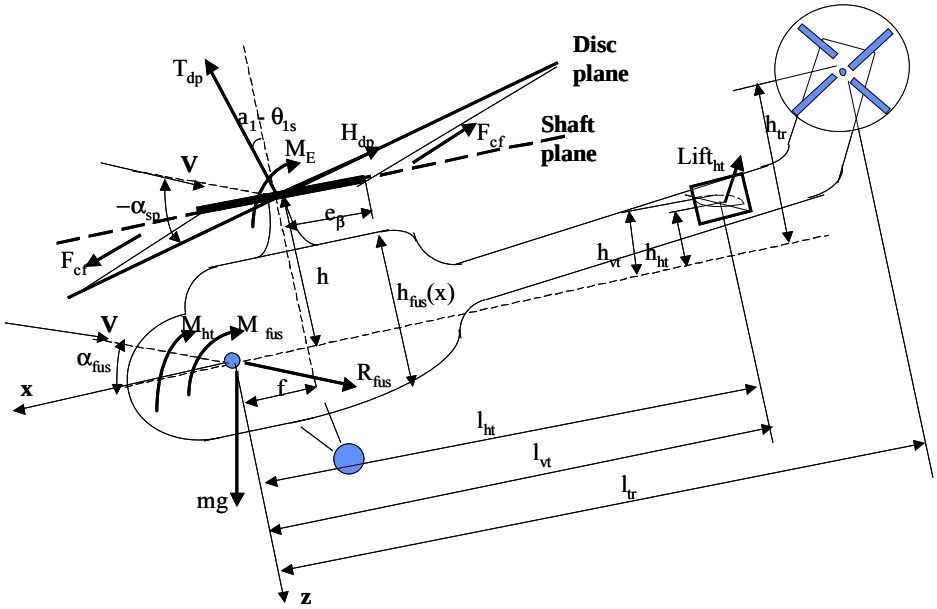

Lateral view

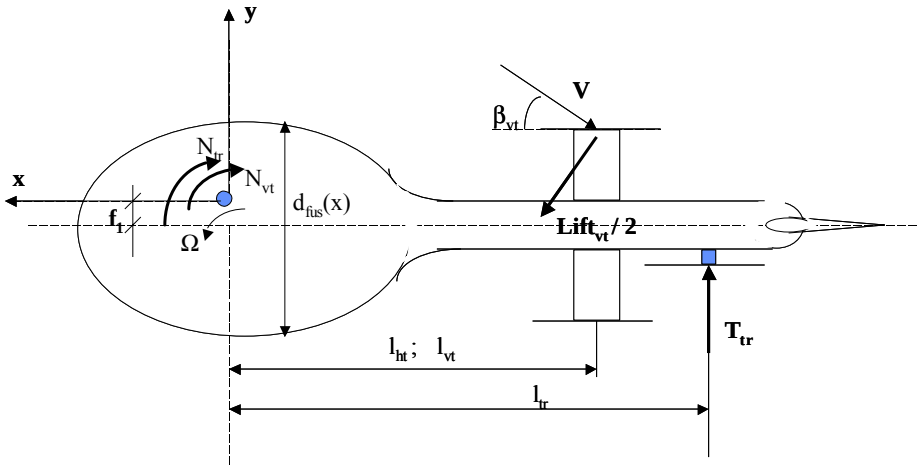

Top view

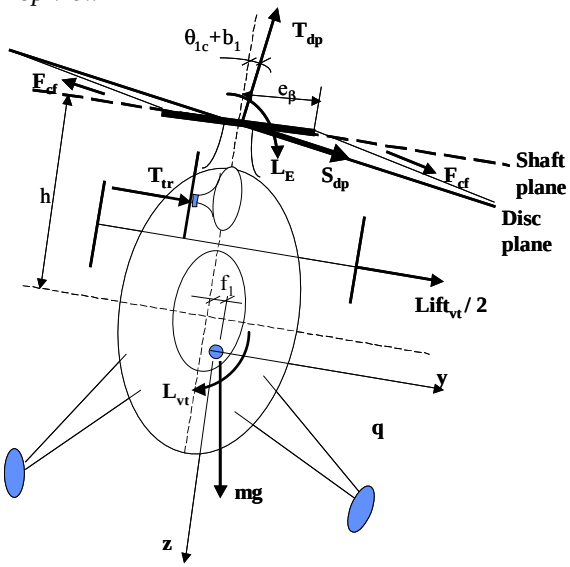

Aft view

Figure A2: Helicopter forces and moments on its main components